

A Biomimetic Honeycomb-like Scaffold Prepared by Flow-focusing Technology for Cartilage Regeneration[†]

Chen-Chie Wang^{1,2}, Kai-Chiang Yang^{3,4}, Keng-Hui Lin⁵, Chang-Chin Wu^{6,7}, Yen-Liang Liu⁸, Feng-Huei Lin⁸, Ing-Ho Chen^{2,9*}

1. Department of Orthopedic Surgery, Taipei Tzu Chi Hospital, The Buddhist Tzu Chi Medical Foundation, New Taipei City 23142, Taiwan
2. Department of Orthopedics, School of Medicine, Tzu Chi University, Hualien 97004, Taiwan
3. School of Dental Technology, College of Oral Medicine, Taipei Medical University, Taipei Medical University, Taipei 11031, Taiwan
4. Department of Organ Reconstruction, Institute for Frontier Medical Sciences, Kyoto University, Kyoto 606-8507, Japan
5. Institute of Physics and Research Center for Applied Science, Academia Sinica, Taipei 11529, Taiwan
6. Department of Orthopedics, National Taiwan University Hospital, College of Medicine, National Taiwan University, Taipei 10002, Taiwan
7. Department of Orthopedics, En Chu Kong Hospital, New Taipei City 23702, Taiwan
8. Institute of Biomedical Engineering, College of Engineering and College of Medicine, National Taiwan University, Taipei 10031, Taiwan
9. Department of Orthopedic Surgery, Hualien Tzu Chi Hospital, The Buddhist Tzu Chi Medical Foundation, Hualien 970, Taiwan

* Address for correspondence: Ing-Ho Chen, MD.

Associate Professor, School of Medicine, Tzu Chi University, No. 707, Sec. 3, Chung Yang Rd., Hualien 97004, Taiwan

TEL: (+886)-3-8561825

FAX: (+886)-3-8560977

E-mail: ing.ho@msa.hinet.net

[†]This article has been accepted for publication and undergone full peer review but has not been through the copyediting, typesetting, pagination and proofreading process, which may lead to differences between this version and the Version of Record. Please cite this article as doi: [10.1002/bit.25295]

Additional Supporting Information may be found in the online version of this article.

© 2014 Wiley Periodicals, Inc.

Received February 28, 2014; Revision Received April 30, 2014; Accepted May 14, 2014

Abstract

A tissue engineering chondrocytes/scaffold construct provides a promise to cartilage regeneration. The architecture of a scaffold such as interconnections, porosities and pore sizes influences the fates of seeding cells including gene expression, survival, migration, proliferation, and differentiation thus may determine the success of this approach. Scaffolds of highly ordered and uniform structures are desirable to control cellular behaviors. In this study, a newly designed microfluidic device based on flow-focusing geometry was developed to fabricate gelatin scaffolds of ordered pores. In comparison with random foam scaffolds made by the conventional freeze-dried method, honeycomb-like scaffolds exhibit higher swelling ratio, porosity, and comparable compressive strength. In addition, chondrocytes grown in the honeycomb-like scaffolds had good cell viability, survival rate, glycosaminoglycans production, and a better proliferation than ones in freeze-dried scaffolds. Real-time PCR analysis showed that the mRNA expressions of aggrecan and collagen type II were up-regulated when chondrocytes cultured in honeycomb-like scaffolds rather than cells cultured as monolayer fashion. Oppositely, chondrocytes expressed collagen type II as monolayer culture when seeded in freeze-dried scaffolds. Histologic examinations revealed that cells produced proteoglycan and distributed uniformly in honeycomb-like scaffolds. Immunostaining showed protein expression of S-100 and collagen type II but negative for collagen type I and X, which represents the chondrocytes maintained normal phenotype. In conclusion, a highly ordered and honeycomb-like scaffold shows superior performance in cartilage tissue engineering.

Keywords: cartilage tissue engineering; gelatin; flow-focusing; microfluidic; scaffold.

1. Introduction

Articular cartilage is known to have limited capacity for self-regeneration. Minor trauma may lead to progressive damage and degeneration of cartilage. Conservative treatments for chondral or osteochondral lesions involve non-weight bearing of the limb for six weeks to three months, corticosteroid injection, and external bone stimulation (Harada et al., 2002). Patients with persistent symptoms are advised to receive further operative treatment. A bone marrow stimulating procedure is often attempted before more invasive surgery, especially in small chondral or osteochondral lesions. Pridie's procedure (subchondral drilling), abrasion arthroplasty, and microfracture are all bone marrow stimulating methods used to recruit mesenchymal stem cells from subchondral bone for cartilage regeneration (Sgaglione, 2005). The main shortcoming of these approaches is that the defect is repaired by fibrocartilage, which has less ability to absorb shock and decrease shear force around the synovial joint (Hangody et al., 2008). As mentioned above, the uneven loading of the cartilage will lead to later osteoarthritic change, and the results of bone marrow stimulating methods will diminish over time. Mosaicplasty and autogenous chondrocyte transplantation (ACT) are new options, but gap existence between the regenerated and host tissues and fibrocartilage formation are still problems (Minas et al., 2000).

Besides ACT procedures, implantation of a chondrocytes/scaffold construct is an alternative. This tissue engineering approach promises a new way for cartilage regeneration by culturing cells in a scaffold with appropriate signal molecules. Among these factors, the three-dimensional (3D) architecture of scaffold was shown the important factor for the biological performances of seeding cells. To provide a 3D structure mimicking the cell growth environment, many kinds of scaffold architectures have been made via different manufacturing processes such as freeze-dried, electrospinning, phase separation, gas foaming, solvent casting, and particulate leaching (Dehghani et al., 2011; Annabi et al., 2010). However, most of these methods generate unequal pore sizes and the interconnected pore may be impeded without a good connection. It has been reported that the pore size influences cell viability, migration, proliferation, and redifferentiation (Stenhamre et al., 2011; Miot et al., 2005). To decrease the interference of the structure, highly ordered and uniform spatial structures are desirable (Dai et al., 2010; Hahn et al., 2006).

In order to obtain scaffold with uniform pore size, new approaches such as two-photon laser scanning

photolithography, 3D printing/rapid prototyping, and sphere-templating were developed (Hsieh et al., 2010; Lee et al., 2012; Ma and Choi, 2001). However, disadvantages such as expensive robotic control and time-consuming pixel-by-pixel writing are remaining. Previously, a self-assembly approach using microfluidic technology was reported to prepare scaffolds (Chung et al., 2009). This low-cost technique can fabricate a scaffold with a highly organized structure and uniform pore size efficiency (Wang et al., 2011). In this study, a new designed microfluidic device constructed by flow-focusing theory was used to prepare gelatin microbubbles, and the application of this gelatin scaffold in cartilage tissue engineering was assessed.

Materials and Methods

Flow-focusing microfluidic device for scaffold fabrication

The flow-focusing microfluidic device was composed of a two-channel glass tube equipped with a micropipette and one capillary over the bottom was used in this study (Fig. 1A). A polyethylene (PE) tube was connected from the upper orifice to a nitrogen gas bottle. Another PE tube was connected a syringe to the lower orifice of the microfluidic device for aqueous solution injection. The micropipette was made from a cylindrical capillary tube (B100-75-10, Shutter Instrument, USA), pulled by a micropipette puller (P-97, Sutter Instrument, USA), and nestled within the other capillary whose inner diameter was close to the outer diameter of the cylindrical tube (BF200-156-10, Shutter Instrument, USA) (Fig. 1 B).

A gelatin type A powder (A1890, Sigma-Aldrich, St. Louis, Mo, USA) was dissolved in 0.1 N acetic acid with 0.5% Pluronic[®] F127 (Sigma, P2443-250G) surfactant at 50°C. The gelatin solution (8%) was filtered with a 0.22 μ m filter (Millex-GV, Millipore, USA) for sterilization. The gelatin solution was put into the 20cc syringe and pumped by the syringe pump (PHD 22/2000, Harvard Apparatus, USA). Nitrogen gas and aqueous gelatin solution were pumped through the upper and the lower channels in the opposite direction, respectively. Uniform microbubbles were generated under a controlled flow rate (200 μ L/min) controlled by the syringe pump and gas pressure (5 psi) measured by a digital pressure indicator (PM, Heise, USA).

The microbubbles were collected and inspected by an invert microscope. When microbubbles were organized in ordered arrays, microbubbles were highly homogeneous. The collected microbubbles were then placed at -20°C for 30 min for gelation and subsequently immersed in a 1% glutaraldehyde solution (Sigma,

G6257) for cross-linking at 4°C for 12 h. The gelled foam was then put in the vacuum system overnight to open up pores and remove air. The obtained scaffolds were then immersed in 0.5 M glycine solution for 1 h; the procedure was repeated 3 times to quench the residual cross-linkers.

A dermal punch was used to cut the scaffold blocks into uniform cylindrical scaffolds (5mm in diameter and 5mm in length) in a sterile condition. Next, the cut gelatin scaffolds were immersed in 5% antibiotic solution (P4083, Sigma-Aldrich) for 1 h. The microfluidic scaffolds were stored in sterilized phosphate buffered saline (PBS) containing 1% antibiotics at 4°C.

Confocal laser scanning microscope observation for the scaffold

Fluorescein isothiocyanate (FITC, F7250, Sigma-Aldrich) at 0.2 mg/mL was added to the gelatin solution to facilitate the observation of microstructure. The gelatin solution containing FITC was used to prepare scaffolds as previously described and observed using a confocal laser scanning microscope (TCS-SP5, Leica, Bannockburn, IL).

Swelling ratio, porosity and compressive strength of the scaffold

The swelling ratio and porosity of this microbubbles scaffold were determined, and a traditional gelatin scaffold was prepared by the freeze-dried method for comparative purposes (Chiang et al., 2012). Briefly, a 8% gelatin solution was cross-linked in 1% glutaraldehyde solution at 4°C for 12 h. The cross-linked samples were frozen overnight, lyophilized for 72 h, and treated with glycine solution to remove the residual cross-linkers. Finally, the freeze-dried scaffolds were immersed in antibiotic solution for sterilization.

The wet scaffolds were weighed (W_t) first, and the scaffolds were dried in a freeze dryer. Dried scaffolds were weighed (W_0) again. The swelling ratio Q was defined as W_t/W_0 . The porosity of the scaffolds was measured according to Archimedes' principle, and was calculated using the following formula: porosity = $((W_2 - W_1)/(W_2 - W_3)) \times 100\%$, where W_1 is the weight of the sample in air, W_2 is the weight of the sample with water, and W_3 is the weight of the sample suspended in water.

The compressive strength of the microfluidic or freeze-dried scaffolds was tested with an Instron 4505 mechanical tester with 10 kN load cells following the guidelines in ASTM D5024-95a. The crosshead speed

was set at 0.4 mm/min, and load was applied until the specimens were compressed to approximately 30% of the original thickness. Compressive modulus was calculated as the slope of the initial linear portion of the stress-strain curve.

Chondrocyte harvesting, culturing, and seeding

Articular cartilage was harvested from porcine hind leg, and chondrocytes were isolated as a previous study (Wang et al., 2011). Cells were cultured in Dulbecco's modified eagle's medium (DMEM, SH30003.01, Hyclone, Logan, UT) supplemented with 50µg/ml L-ascorbic acid (A5960, Sigma-Aldrich), 10% fetal bovine serum (100-106, Gemini Bio-Products, USA), and 1% antibiotic in an incubator set at 5% CO₂ and 95% humidity at 37°C. At 70-80% confluency, the cells (passage 3-5) were collected, re-suspended in medium (5x10⁶ cells/mL), and seeded into the microfluidic or freeze-dried scaffolds using a 24 gauge needle. Each scaffold contained 2x10⁵ cells with 50 µL medium. The cells/scaffold construct was first placed in an incubator for 1 h for cell adhesion, and then transferred to a 12-well culture plate. Finally, medium was added, and culture medium was changed every 2 days.

Cell proliferation, activity and cytotoxicity test

Total DNA quantification was used to determine the cell proliferation. Chondrocytes/microfluidic or freeze-dried scaffolds (n=12 for each scaffold) were divided into 3 subgroups and cultured for 1, 3, and 5 days for DNA quantification. The cells/scaffold constructs were digested in papain solution (P4762, Sigma-Aldrich) at 60°C for 16 h. Total DNA of the digested sample was extracted using a DNeasy Blood and Tissue kit (69504, QIAGEN, Germany). The amount of DNA was measured by the NanoDrop spectrophotometer.

The activity of the chondrocytes in scaffolds was evaluated using a water-soluble tetrazolium salt-1 assay (WST-1, K301-2500, Biovision, CA, USA). Prior to treatment, culture medium was aspirated for further cytotoxicity evaluation and then cells/scaffolds were washed with PBS. DMEM containing 10% WST-1 agent was added and incubated for a further 2.5 h. The result of the WST-1 assay was determined by a spectrophotometer (SunriseTM, Tecan, Switzerland) at the wavelength of 460 nm. For evaluation of cytotoxicity, the aspirated medium before WST-1 test was reacted with a lactate dehydrogenase assay (LDH assay, G1780,

Promega, USA). The result of the LDH assay was measured by the spectrophotometer at the wavelength of 450 nm.

Cell survival study

After being cultured for 7 days, chondrocytes in microfluidic scaffolds were underwent live staining in media containing calcein-AM (C3099, Invitrogen Corp.) for 30 min to assess cell survival (Yang et al., 2013). The chondrocytes/microfluidic scaffold constructs were subsequently stained with 2 $\mu\text{mol/L}$ of DAPI (sc-3598, Santa Cruz Biotechnology, USA) for 7 min. After treatment, the cells/scaffolds were observed using a fluorescent microscopy (HAL 100/HBO 100, AxioCam MRc5, Zeiss, Germany).

Glycosaminoglycan production

The glycosaminoglycan (GAG) production was evaluated by a 1,9-dimethyl-methylene blue (DMMB, 341088, Sigma-Aldrich) assay. Cells cultured in monolayer fashion and cells/scaffolds constructs (n=12 for each scaffold) were digested in papain solution as previous section after being cultured for 1, 2, and 3 weeks, and the digested sample was reacted with DMMB reagent. The GAG content of blank scaffolds that underwent identical culture periods as study groups was used for background subtraction. Chondroitin-6-sulfate (C4384, Sigma-Aldrich) was used to establish a standard curve with sequential dilution. Absorbance was detected at a wavelength of 595 nm by a microplate reader. The cell number was quantified using total DNA as previous section, and the GAG production was normalized based on the cell number of each group.

mRNA expression of chondrocytes (real-time PCR)

Total RNA of monolayer culture, chondrocytes/microfluidic and freeze-dried scaffold constructs were extracted (RNA mini-kit, Quiagen), and RNA quantity and purity were determined using a spectrophotometer. The cDNA was synthesized from RNA using Superscript II RT (18064-014, Invitrogen). Aggrecan, collagens type I, II, and X were chosen as target genes to analyze the gene expression (Wang et al., 2012). Glyceraldehyde-3-phosphate dehydrogenase (GAPDH) was used as an endogenous housekeeping gene. The PCR reaction was performed with an ABI PRISM 7900 Sequence Detection System with Sequence Detection Software 1.9.1. The relative expression of each target gene was examined using the $2^{-\Delta\Delta\text{Ct}}$ method.

Histologic examination

The chondrocytes/microfluidic scaffold constructs were fixed in a 10% neutral buffer formalin solution after 3 weeks of culture. The construct was dehydrated in a graded series of ethanol and embedded in paraffin wax. Consecutive sections were cut from the paraffin blocks into 5 μm slides. The sections were deparaffinized and stained with hematoxylin and eosin (H&E) to assess the cells/scaffold morphology. Toluidine blue staining was used to determine GAG production. For the immunohistochemical (IHC) staining, the sections were first immersed in a methanol solution with 3% H_2O_2 for 10 min to quench the endogenous peroxidase activity, and then pre-incubated with serum blocking solution for 20 min to block the non-specific binding. The sections were labeled with streptavidin-biotin (85-8943, Histostain-Plus, Invitrogen, CA, USA) following incubation with anti-S-100 antibody (Novocastra Laboratories Ltd, Newcastle upon Tyne, UK) at room temperature for 2 h. Other sections were incubated overnight with anti-collagen type I antibody (CSI 008-01-02, Thermo, IL, USA), anti-collagen type II antibody (PAB13494, Abnova, Taipei, Taiwan), and anti-collagen type X antibody (ab49945, Abcam, Cambridge, UK). The presence of the antigen was indicated by a brown color with 3, 3'-diaminobenzidine (00-2014, Invitrogen, CA, USA). The sections were further counter-stained with hematoxylin. Negative controls were processed identically, except that the primary antibodies were replaced with IgG.

Statistical analysis

Data was expressed as mean \pm SEM. Statistical analyses of swelling ratio, porosity, compressive strength, cell activity, cytotoxicity, GAG contents, total DNA, and real-time PCR were analyzed by ANOVA analysis with a post-hoc Dunnett's multiple comparison tests. Difference was considered significant when the p-value was less than 0.05.

Results

Characterization and observation of the scaffold

The prepared microfluidic scaffolds are shown in Fig. 2A. The bubble size was controlled by air pressure and liquid flow rate in the microfluidic device, and uniform bubbles were generated and collected to form the

scaffold (Fig. 2B). After the vacuum degassing process, the interconnected pores were created due to the pressure difference in the scaffold and outside break the walls around the pores. Confocal microscopy showed the microbubbles self-assembled layer by layer, reconstituting a highly organized 3D ordered array (Fig. 2C) with a highly organized honeycomb-like structure (Fig. 2D). An interconnecting porous structure was also shown in the gelatin scaffold under confocal microscopy (Fig. 2E).

Swelling ratio, porosity and compressive strength of the scaffold

The average swelling ratio was $2607.41 \pm 340.10\%$ in the microfluidic scaffold compared with $523.09 \pm 58.74\%$ in the freeze-dried scaffold ($p < 0.01$, Table 1). The average porosity was $97.25 \pm 0.84\%$ in the honeycomb-like scaffold, which was significantly higher than that of the traditional gelatin scaffold ($85.09 \pm 1.51\%$), ($p < 0.05$). The compressive strength was 765 ± 32 KPa for the freeze-dried gelatin scaffold and 720 ± 25 KPa for the microfluidic scaffolds. No significant difference was noticed between these two groups.

Cell seeding, activity, cytotoxicity test, and cell proliferation

Chondrocyte seeding in the honeycomb-like scaffold was investigated directly using an optical microscope due to the transparent character of the scaffold. Fig. 3A represents cells seeded in the microfluidic scaffold and cultured for 3 days. The chondrocytes grow fast and aggregated in the microfluidic scaffold (Fig. 3B), and the pores were filled with cells (Fig. 3C). However, cells were unable to be seen directly under optical microscope when seeded in the freeze-dried scaffolds.

The amount of DNA, which indicates the cell number, was increased significantly ($n=6$, $p < 0.05$) at day 3 from day 1, which reveals chondrocytes proliferated well in both microfluidic and freeze-dried scaffolds (Fig. 3D). The DNA content of the honeycomb-like scaffolds was significantly higher than that of the freeze-dried scaffolds at day 5 ($n=6$, $p < 0.05$). There was no significant difference in DNA content between day 3 and day 5 for the freeze-dried scaffolds.

The activity of chondrocytes cultured in both types of gelatin scaffolds increased with the length of the culture periods (Fig. 3E). The activity of cells cultured in the honeycomb-like scaffolds was significantly higher than that of the freeze-dried scaffolds ($n=6$, $p < 0.05$). The cell toxicity was also slightly increased with the length of the culture periods, which presents normal cell death under culture (Fig. 3F). The cytotoxicity of cells

in the freeze-dried gelatin scaffolds was slightly higher than that of cells in the honeycomb-like scaffolds (n=6, p<0.05 at day 3).

Cell survival study

Live staining showed the cells survived well in the microfluidic scaffolds. In Fig. 4, the color blue represents the cell nucleus, the color green represents the live cells, and the color red represents the gelatin scaffold. On day 7, the cells were distributed uniformly on the wall of the microfluidic scaffold (Fig. 4A and D); most cells were stained with green fluorescence (Fig. 4B and E) and the merged images (Fig. 4C and F) show that cells had a good survival ratio.

Glycosaminoglycan production

The GAG production of chondrocytes cultured in the honeycomb-like scaffolds at week 2 was significantly higher than that of week 1 (n=6, p<0.05, Fig. 5), and the GAG productions at week 1 and 2 were also significantly higher than cells in freeze-dried scaffolds at the same time points (n=6, p<0.05). Although the production decreased at week 3, cells cultured in honeycomb-like scaffolds still had a higher GAG production relative to freeze-dried scaffolds (n=6, p<0.05). However, cells cultured in monolayer fashion had low and constant GAG productions that were lower than cells in scaffolds significantly.

mRNA expressions

For chondrocytes cultured in freeze-dried scaffolds, the expression of aggrecan was up-regulated at week 1 but restored to normal level at week 2 and 3 (without significant difference, Fig. 6). The collagen type I was down-regulated with significant difference (p<0.01) while collagens type II and X were not influenced relative to cells cultured in monolayer fashion (Fig. 6A). For cells cultured in the microfluidic scaffolds, the expression of aggrecan increased at week 1, and collagen type II were increased significantly through the experiment (p<0.05). On the other hand, collagen type I decreased at week 2 and week 3 (p<0.05). For collagen type X, the mRNA expression increased slightly at week 1, but was restored to a normal level at week 2 and week 3.

Histologic examination

H&E staining showed the cells distributed uniformly in the microfluidic scaffolds after 3 weeks of culture (Fig. 7A). The proteoglycan produced by the chondrocytes was proved through toluidine blue staining (Fig. 7B). The chondrocytes retained their round-shaped morphology and positivity for S-100 protein staining (brown color, IHC for S-100, Fig. 7C). Collagen type I is the most abundant collagen in the human body and can also be found in abnormal fibrocartilage. Negative staining meant the chondrocytes from the porcine hyaline cartilage were able to keep their phenotype (Fig. 7D). In this case, the chondrocyte/gelatin scaffold was positivity for collagen type II staining (brown color, IHC for collagen type II, Fig. 7E). Collagen type X is found in hypertrophic and mineralizing cartilage. Fig. 7F shows the negative staining in the samples, which revealed the chondrocytes were not transformed into hypertrophic phenotype.

Discussion

The architecture and pore geometry of scaffolds not only determine the mechanical properties of scaffolds but also influence the cellular behaviors of seeding cells (Woodfield et al., 2004; Moroni et al., 2006). The microstructure has been contemplated as playing an important role in cell growth and extracellular matrix (ECM) production in tissue engineering (Hutmacher et al., 2000). It also influences cell seeding efficiencies (Lu et al., 2010). A porous structure with adequate pore size provides space for cell attachment, growth, and matrix production (Lien et al., 2009). The diameter of the interconnecting pore affects cell migration, nutrient supply, and metabolic waste removal (Stenhamre et al., 2011; Miot et al., 2005). Traditional methods for scaffold fabrication generate unequal pore size, impediment interpores, and closed surface structures (Ko et al., 2010). Based on above studies, a highly ordered and uniform scaffold shall benefit the development of tissue engineering. A more organized microstructure could provide greater biomechanical strength (Zhang et al., 2005; Wu et al., 2010). Zhang et al. compared scaffolds fabricated by the unidirectional freeze-dried method and the conventional freeze-dried method; their results showed that unidirectional freeze-dried produced better biomechanical strength (Zhang et al., 2007). The scaffold made using the unidirectional freeze-dried method could stand a higher compression force from the longitudinal direction than from the transverse direction. This was attributed to all the walls of the microtubes supporting the force along the longitudinal direction (Wu et al., 2010). Our scaffold has a hexagonal close-packed crystal-like structure that resembles a bee honeycomb framework; it is characterized by substantial rigidity in shear, high crushing stress, and has a light and relative

insensitivity to local loss of stability. This honeycomb-like scaffold was structured self-assembly during microbubble stacking. The structure was proved to possess the highest fraction of spaces occupied by equal size spheres. In comparison with the unidirectional freeze-dried method, a scaffold constructed with columnar architecture and the hexagonal structure only speculated at cross-section perpendicular to the microtubes, the hexagonal composition of this scaffold can be viewed in 3 directions and thus possessed similar biomechanical force. This honeycomb-like scaffold was fitted out with a suitable microstructure as well as mechanical strength.

The swelling ratio of honeycomb-like scaffold is 5 times higher than freeze-dried scaffolds, which may attribute to the monodispersed scaffold was produced with less material and constructed with a thin wall rather than a freeze-dried scaffold. Another possible mechanism is that the highly organized, uniform constructs possessed microbubbles stacked hierarchically in an outward direction without impedance. Conventional techniques for fabricating scaffold generate pores with a wide distribution in size and shape, and these pores could not expand thoroughly when immersed in the liquid. The porosity of a honeycomb-like scaffold is significantly higher than the porosity of a freeze-dried scaffold. In addition to the inherently high porosity and highly organized construct, conventional scaffold may have more closed cells in the scaffold since some interpores are not created during the fabricating process. Closed cells are characterized by a limited compression and expansion capacity, which also limits cell migration/distribution. Interconnected pores provide more efficient fluid circulation between pores. Cells cultured in the scaffold are well nourished with supply oxygen and other nutrients and exchange of CO₂ and other metabolic waste products.

It has been shown that different cells have their preferred pore sizes in 3D culture conditions (Griffon et al., 2006; Yamane et al., 2007). Scaffold with a larger pore size may lead to lower cell attachment onto the inner walls and decrease intracellular signaling. A small pore size was suggested to inhibit cell penetration and metabolic activity (Cao et al., 1998). For chondrocyte culture, a pore size between 250-500µm provides a relatively appropriate environment for cell growth and promotes ECM production (Lien et al., 2009). Considering the normal cell phenotype maintaining, cell distribution, and mechanical strength of scaffold, the choice of pore size for scaffold fabrication is on the horn of a dilemma.

In order to ensure the uniform cellular distribution in the scaffold, the cells/medium suspensions were injected into multiple positions of a scaffold. However, we noticed that most cells attached to the internal

surface of scaffold at the beginning of experiment. After that, cells began to fill the entire space of pore as cells proliferation. As shown in Fig. 4, the peripheral part of scaffold was filled with cells. Oppositely, most cells were found to adhere on the surface predominantly in the central area of the scaffolds. For the growth of chondrocytes, the DNA contents increased in both types of gelatin scaffolds by day 3 from day 1. However, the DNA content of the freeze-dried gelatin scaffolds leveled off from day 3 to day 5, which means stalled cell proliferation. On the other hand, the DNA contents of the honeycomb-like scaffolds continually increased to day 5, proving that there is more space for cell growth in an ordered scaffold than a freeze-dried one. We assume the chondrocytes still proliferate and shall fill the entire space eventually. Even though the DNA contents were similar at day 1 and day 3 for both scaffolds, cell activity in the honeycomb-like scaffold was higher than that in the freeze-dried scaffold. The architecture of scaffold further influenced GAGs production of chondrocytes. Chondrocytes cultured in the microfluidic scaffolds showed better cell proliferation and higher GAGs productions. On the contrary, cells cultured in monolayer fashion proliferated fast with low GAGs contents. Haugh et al. found the crosslinking and mechanical properties of scaffolds influence cell attachment, proliferation, and migration (Haugh et al., 2011). The scaffold stiffness was also reported to influence proliferation and biosynthesis of chondrocytes (Lee et al., 2001). The substrate stiffness and the degree of cross-linking of honeycomb-like scaffolds were different from those of freeze-dried scaffolds, which may provide a possible explanation for our findings.

The materials used for cartilage tissue engineering influence the gene expression pattern of chondrocytes dramatically (Freyria et al., 2009; Tsai et al., 2006). A drawback of using the alginate scaffold for cartilage tissue engineering was the up-regulation of collagen type X (Wang et al., 2012). Calcium ions used for alginate gelation may induce chondrocytes hypertrophic change and transform to osteogenesis (Chang et al., 2002). This cell differentiation to hypertrophic chondrocytes is irreversible, even with further culturing in a 3D collagen type II sponge (Mukaida et al., 2005). However, we did not observe this phenotype change in gelatin scaffolds. Even though the collagen type X was slightly increased by week 1 relative monolayer cells, the expression decreased to a normal level. Moreover, the mRNA expression of aggrecan increased during whole culture periods, which was not reported when the alginate scaffolds were used. Aggrecan is the functional component of cartilage and its polyanionic character attracts water, which allows the cartilage to swell. Several studies have reported a slight decrease in aggrecan for cells cultured in a 3D scaffold (Wu et al., 2012), but

chondrocytes expressed up-regulation of aggrecan in the microfluidic scaffolds. Another interesting finding is the collagen type II; though both the raw materials of freeze-dried and microfluidic scaffold were gelatin, the expressions of collagen type II were highly up-regulated in the later one only. In addition, the collagen type I was down-regulated during the experimental periods. These results suggested the chondrocytes kept the phenotype without transforming to fibroblast, fibrocartilage or osteoblast in the honeycomb-like scaffolds.

Although the protein production pattern of chondrocytes in the freeze-dried scaffolds (Supplementary Material 1) was similar to those in the honeycomb-like scaffolds, many chondrocytes migrated to the surface of freeze-dried scaffolds (Supplementary Material 1a). Because of the oxygen/nutrition gradient, the seeding cells may migrate to the boundary of the scaffold, and the center of the scaffold may have fewer cells which is a well-known problem of tissue engineering (Wu et al., 2012). On the contrary, the histological examinations showed the chondrocytes distributed more uniformly within the honeycomb-like scaffolds, and the toluidine blue staining indicated that cells produced the cartilage matrix. In general, a lack of S-100 expression indicated that the chondrocytes had lost their phenotype. Collagen type II, a major component of hyaline cartilage, is produced by functional and healthy chondrocytes only. The IHC staining revealed collagen type II and S-100 proteins in the chondrocytes/gelatin scaffolds which indicated the porcine chondrocytes had maintained their functional phenotypes (Fan et al., 2014). In addition, the cells/scaffold was negative for collagen type I and X staining. Chondrocytes produce collagen type I may represent the trans-differentiation to fibrocartilage. Collagen type X is expressed when chondrocytes become hypertrophic and the cells gradually differentiate toward osteogenesis (Mukaida et al., 2005). In combination with the findings of mRNA expressions, these results demonstrated that ordered gelatin scaffolds maintain chondrocytes in healthy phenotypes. Another noticeable finding is the ECM production, both toluidine blue and type II collagen staining revealed that most of the ECMs were deposited in the pericellular area but not within the space of scaffolds. Using a porous alginate scaffold, Lin et al. reported the 3D culture enhanced chondrocytes' matrix synthesis (Lin et al., 2009). However, considering the cell proliferation, the GAG production of cells was not increased actually. The increase of ECM production was disproportionate to cell proliferation. According to our experiences, though chondrocytes maintain normal phenotype under 3D culture, and the collagen as also as GAG productions are better than those of 2D culture. We assume that chondrocytes prefer proliferation rather than ECM deposition in a 3D scaffold until whole space is filled with cells.

It has been known that the transcription factor Sox9 up-regulates the expressions of aggrecan and collagen II in chondrocytes, and this is contributed to the transforming growth factor-beta (TGF- β) signaling results in the up-regulation of Sox9 (Chen et al., 2008). To sum up, we speculate that the honeycomb-like scaffold may regulate TGF- β and subsequent regulate the Sox9 expression since the scaffold stiffness influence the cell adhesion and cytoskeletal tension (Wang et al., 2012). It may provide more information to demonstrate whether the structure or stiffness of scaffold influences the TGF- β signaling pathway and proliferative markers.

This technology has the potential of application in other fields of tissue regeneration research, since the pore size can be easily adjusted by air pressure, fluid velocity and the micropipette tip diameter of the microfluidic device. The architecture of this honeycomb-like scaffold is similar to the pulmonary alveolus (Zhang et al., 2011), thus this approach may also be used in to reconstruct an alveolus-like structure for lung tissue engineering in the future.

Conclusion

The honeycomb-like scaffold prepared by a flow-focusing microfluidic device overcomes obstacles, such as inconsistent pore size and impeded interconnecting pores in traditional scaffold. The highly organized structure was observed to resemble a bee honeycomb framework with a hexagonal close-packed microstructure. Moreover, when the gelatin scaffold used in chondrocytes' culture, cells maintained normal phenotype with functional ECM proteins production. The honeycomb-like scaffolds provide promising routes for cartilage regeneration.

Acknowledgement

This research was supported by National Science Council, Taiwan under Grant NSC102-2320-B-303-001-MY3.

The authors would like to thank Ching-Yen Lin, Ya-Yun Yang, and Ya-Ting Yang for the assistances of SEM examination in the Instrumentation Center at National Taiwan University.

Conflict of interest

The authors confirm that there are no conflicts of interest.

References

- Annabi N, Nichol JW, Zhong X, Ji C, Koshy S, Khademhosseini A, Dehghani F. 2010. Controlling the porosity and microarchitecture of hydrogels for tissue engineering. *Tissue Eng Part B Rev* 16:371-383.
- Chang W, Tu C, Pratt S, Chen TH, Shoback D. 2002. Extracellular Ca(2+)-sensing receptors modulate matrix production and mineralization in chondrogenic RCJ3.1C5.18 cells. *Endocrinology* 143:1467-1474.
- Chiang TS, Yang KC, Zheng SK, Chiou LL, Hsu WM, Lin FH, Huang GT, Lee HS. 2012. The prediction of drug metabolism using scaffold-mediated enhancement of the induced cytochrome P450 activities in fibroblasts by hepatic transcriptional regulators. *Biomaterials* 33:5187-5197.
- Chen YL, Chen HC, Chan HY, Chuang CK, Chang YH, Hu YC. 2008. Co-conjugating chondroitin-6-sulfate/dermatan sulfate to chitosan scaffold alters chondrocyte gene expression and signaling profiles. *Biotechnol Bioeng* 101:821-830.
- Chung KY, Mishra NC, Wang CC, Lin FH, Lin LH. 2009. Fabricating scaffolds by microfluidics. *Biomicrofluidics* 3:022403.
- Dai W, Kawazoe N, Lin X, Dong J, Chen G. 2010. The influence of structural design of PLGA/collagen hybrid scaffolds in cartilage tissue engineering. *Biomaterials* 31:2141-152.
- Dehghani F, Annabi N. 2011. Engineering porous scaffolds using gas-based techniques. *Curr Opin Biotechnol* 22:661-666.
- Fan FY, Chiu CC, Tseng CL, Lee HS, Pan YN, Yang KC. 2014. Glycosaminoglycan/chitosan hydrogel for matrix-associated autologous chondrocyte implantation: An in vitro study. *J Med Biol Eng* doi: 10.5405/jmbe.1516.
- Freyria AM, Ronzière MC, Cortial D, Galois L, Hartmann D, Herbage D, Mallein-Gerin F. 2009. Comparative phenotypic analysis of articular chondrocytes cultured within type I or type II collagen scaffolds. *Tissue Eng Part A* 15:1233-1245.
- Griffon DJ, Sedighi MR, Schaeffer DV, Eurell JA, Johnson AL. 2006. Chitosan scaffolds: interconnective pore size and cartilage engineering. *Acta Biomater* 2:313-320.
- Hahn MS, Miller JS, West JL. 2006. Three-dimensional biochemical and biomechanical patterning of hydrogels for guiding cell behavior. *Advanced Materials* 18:2679-2684.

- Hangody L, Vásárhelyi G, Hangody LR, Sükösd Z, Tibay G, Bartha L, Bodó G. 2008. Autologous osteochondral grafting--technique and long-term results. *Injury* 39: S32-39.
- Harada Y, Tomita N, Wakitani S, Mii Y, Oka M, Tsutsumi S. 2002. Use of controlled mechanical stimulation in vivo to induce cartilage layer formation on the surface of osteotomized bone. *Tissue Engineering* 8:969-978.
- Haugh MG, Murphy CM, McKiernan RC, Altenbuchner C, O'Brien FJ. 2011. Crosslinking and mechanical properties significantly influence cell attachment, proliferation, and migration within collagen glycosaminoglycan scaffolds. *Tissue Eng Part A* 17:1201-1208.
- Hsieh TM, Ng CW, Narayanan K, Wan AC, Ying JY. 2010. Three-dimensional microstructured tissue scaffolds fabricated by two-photon laser scanning photolithography. *Biomaterials* 31:7648-7652.
- Hutmacher DW. 2000. Scaffolds in tissue engineering bone and cartilage. *Biomaterials* 21:2529-2543.
- Ko YG, Grice S, Kawazoe N, Tateishi T, Chen G. 2010. Preparation of collagen-glycosaminoglycan sponges with open surface porous structures using ice particulate template method. *Macromol Biosci* 10:860-871.
- Lee CR, Grodzinsky AJ, Spector M. 2001. The effects of cross-linking of collagen-glycosaminoglycan scaffolds on compressive stiffness, chondrocyte-mediated contraction, proliferation and biosynthesis. *Biomaterials* 22:3145-3154.
- Lee M, Wu BM. 2012. Recent advances in 3D printing of tissue engineering scaffolds. *Methods Mol Biol* 868:257-267.
- Lien SM, Ko LY, Huang TJ. 2009. Effect of pore size on ECM secretion and cell growth in gelatin scaffold for articular cartilage tissue engineering. *Acta Biomater* 5:670-679.
- Lin YJ, Yen CN, Hu YC, Wu YC, Liao CJ, Chu IM. 2009. Chondrocytes culture in three-dimensional porous alginate scaffolds enhanced cell proliferation, matrix synthesis and gene expression. *J Biomed Mater Res A* 88:23-33.
- Lu H, Ko YG, Kawazoe N, Chen G. 2010. Cartilage tissue engineering using funnel-like collagen sponges prepared with embossing ice particulate templates. *Biomaterials* 31:5825-5835.
- Ma PX, Choi JW. 2001. Biodegradable polymer scaffolds with well-defined interconnected spherical pore network. *Tissue Eng* 7:23-33.
- Minas T, Chiu R. 2000. Autologous chondrocyte implantation. *Am J Knee Surg* 13:41-50.

- Miot S, Woodfield T, Daniels AU, Suetterlin R, Peterschmitt I, Heberer M, van Blitterswijk CA, Riesle J, Martin I. 2005. Effects of scaffold composition and architecture on human nasal chondrocyte redifferentiation and cartilaginous matrix deposition. *Biomaterials* 26:2479-2489.
- Moroni L, de Wijn JR, van Blitterswijk CA. 2006. 3D fiber-deposited scaffolds for tissue engineering: influence of pores geometry and architecture on dynamic mechanical properties. *Biomaterials* 27:974-985.
- Mukaida T, Urabe K, Naruse K, Aikawa J, Katano M, Hyon SH, Itoman M. 2005. Influence of three-dimensional culture in a type II collagen sponge on primary cultured and dedifferentiated chondrocytes. *J Orthop Sci* 10:521-528.
- Sgaglione NA. 2005. Biologic approaches to articular cartilage surgery: future trends. *Orthop Clin North Am* 36:485-495.
- Stenhamre H, Nannmark U, Lindahl A, Gatenholm P, Brittberg M. 2011. Influence of pore size on the redifferentiation potential of human articular chondrocytes in poly(urethane urea) scaffolds. *J Tissue Eng Regen Med* 5:578-588.
- Tsai WB, Chen CH, Chen JF, Chang KY. 2006. The effects of types of degradable polymers were investigated on porcine chondrocyte adhesion, proliferation and gene expression. *J Mater Sci Mater Med* 17:337-343.
- Wang CC, Yang KC, Lin KH, Liu HC, Lin FH. 2011. A highly organized three-dimensional alginate scaffold for cartilage tissue engineering prepared by microfluidic technology. *Biomaterials* 32:7118-7126.
- Wang CC, Yang KC, Lin KH, Liu YL, Liu HC, Lin FH. 2012. Cartilage regeneration in SCID mice using a highly organized three-dimensional alginate scaffold. *Biomaterials* 33:120-127.
- Wang YK, Yu X, Cohen DM, Wozniak MA, Yang MT, Gao L, Eyckmans J, Chen CS. 2012. Bone morphogenetic protein-2-induced signaling and osteogenesis is regulated by cell shape, RhoA/ROCK, and cytoskeletal tension. *Stem Cells Dev* 21:1176-1186.
- Woodfield TB, Malda J, de Wijn J, Péters F, Riesle J, van Blitterswijk CA. 2004. Design of porous scaffolds for cartilage tissue engineering using a three-dimensional fiber-deposition technique. *Biomaterials* 25:4149-4161.
- Wu CC, Huang TL, Liu CC, Lu DH, Yang SH, Yang KC, Lin FH. 2012. The interaction between co-cultured human nucleus pulposus cells and mesenchymal stem cells in a bioactive scaffold. *Process Biochemistry* 47:922-928.

- Wu X, Liu Y, Li X, Wen P, Zhang Y, Long Y, Wang X, Guo Y, Xing F, Gao J. 2010. Preparation of aligned porous gelatin scaffolds by unidirectional freeze-drying method. *Acta Biomater* 6:1167-1177.
- Yamane S, Iwasaki N, Kasahara Y, Harada K, Majima T, Monde K, Nishimura S, Minami A. 2007. Effect of pore size on in vitro cartilage formation using chitosan-based hyaluronic acid hybrid polymer fibers. *J Biomed Mater Res A* 81:586-589.
- Yang KC, Wu CC, Yang SH, Chiu CC, Sumi S, Lee HS. 2013. Investigating the suspension culture on aggregation and function of mouse pancreatic β -cells. *Journal of Biomedical Materials Research: Part A* 101:2273-2282.
- Zhang H, Cooper AI. 2007. Aligned porous structures by directional freezing. *Adv Mater* 19:1529-1533.
- Zhang H, Hussain I, Brust M, Butler MF, Rannard SP, Cooper AI. 2005. Aligned two and three-dimensional structures by directional freezing of polymers and nanoparticles. *Nat Mater* 4:787-793.
- Zhang WJ, Lin QX, Zhang Y, Liu CT, Qiu LY, Wang HB, Wang YM, Duan CM, Liu ZQ, Zhou J, Wang CY. The reconstruction of lung alveolus-like structure in collagen-matrigel/microcapsules scaffolds in vitro. *J Cell Mol Med* 2011;15(9):1878-86.

Figure captions

Figure. 1 Schematic representation of the microfluidic device based on flow-focusing theory. (A) The device was composed a 2-channel glass tube equipped with a micropipette and one capillary over the bottom. A rubber pipe was connected from the upper orifice to a nitrogen gas bottle. Another rubber pipe connected a syringe to the lower orifice of the microfluidic device for aqueous solution injection. (B) The micropipette was made from a cylindrical capillary tube, and nestled within the other capillary whose inner diameter was close to the outer diameter of the cylindrical tube.

Figure. 2 (A) Two gelatin scaffolds prepared by the microfluidic device. (B) Uniform bubbles were generated and collected. (C) Confocal microscopy showed the microbubbles self-assembled layer by layer, (D) reconstituting a highly organized 3D ordered array with a highly organized honeycomb-like structure. (E) Confocal microscopy also showed the microfluidic scaffold had an interconnecting porous structure.

Figure. 3 (A) Chondrocytes were seeded in the microfluidic scaffold and cultured for 3 days. (B) The cells were found to grow numerously and aggregated. (C) The space of the scaffold was filled with cells. (D) The amount of DNA, which represents the cell number, was increased significantly at day 3 relative to day 1, which reveals chondrocytes proliferated well in both kinds of gelatin scaffolds. The DNA content of the microfluidic scaffolds was significantly higher than that of the freeze-dried scaffolds at day 5. No significant difference was noticed in DNA content between day 3 and day 5 for the freeze-dried scaffolds. (E) WST-1 assay revealed that the activity of cells cultured in microfluidic scaffolds was significantly higher than that of the freeze-dried scaffolds. (F) The cytotoxicity of cells in the freeze-dried scaffolds was slightly higher than those in the microfluidic scaffolds.

Figure. 4 The color blue represents the cell nucleus, the color green represents the live cells, and the color red represents the gelatin scaffold. On day 7, the cells distributed uniformly on the wall of the scaffold (A and D); most cells were stained with green fluorescence (B and E) and the merged images (C and F) revealed that cells had a good survival rate.

Figure. 5 Chondrocytes cultured in monolayer fashion had low and constant GAG productions. However, cells in the microfluidic scaffolds had better ability to produce GAGs than those in the freeze-dried scaffolds and monolayer cultures. The GAG production of cells cultured in the honeycomb-like scaffolds at week 2 was significantly higher than that of week 1, and the GAG productions at week 1 and 2 were also significantly higher than cells in freeze-dried scaffolds at the same time points. Although the GAG productions decreased at week 3, cells cultured in honeycomb-like scaffolds still had a higher GAG production relative to the freeze-dried scaffolds.

Figure. 6 (a) Relative to chondrocytes cultured as monolayer fashion, the expression of aggrecan was up-regulated at week 1 when cells cultured in freeze-dried scaffolds. However, the aggrecan expression restored to normal level at week 2 and 3. The collagen type I was down-regulated while collagens type II and X were not influenced. (b) For cells cultured in the microfluidic scaffolds, the expression of aggrecan increased at week 1, and collagen type II were increased significantly through the experiment. On the other hand, collagen type I decreased at week 2 and week 3. For collagen type X, the mRNA expression increased slightly at week 1, but was restored to a normal level at week 2 and week 3.

Figure. 7 (A) H&E staining showed the cells distributed uniformly after 3 weeks of culture in the honeycomb-like scaffolds. (B) Toluidine blue staining proved the chondrocytes produced proteoglycans. (C) IHC staining revealed that the chondrocytes were positivity for S-100 protein staining. (D) Samples were negative for type I collagen staining that represents the chondrocytes were able to keep their phenotype. (E) The cells/microfluidic scaffold was positivity for type II collagen staining, which revealed that the chondrocytes in the scaffold were functioning well. (F) Type X collagen is found in hypertrophic cartilage and results shows the negative staining which revealed the chondrocytes were not transformed into hypertrophic phenotype.

Table 1 Swelling ratio, porosity and compressive strength of the freeze-dried and microfluidic gelatin scaffolds.

	Freeze-dried scaffold (n=4)	Microfluidic scaffold (n=4)
Swelling ratio	523.09±58.74%	2607.41±340.1%
Porosity	85.09±1.51%	97.25±0.84%
Compressive strength	765±32 Kpa	720±25 Kpa

Accepted Preprint

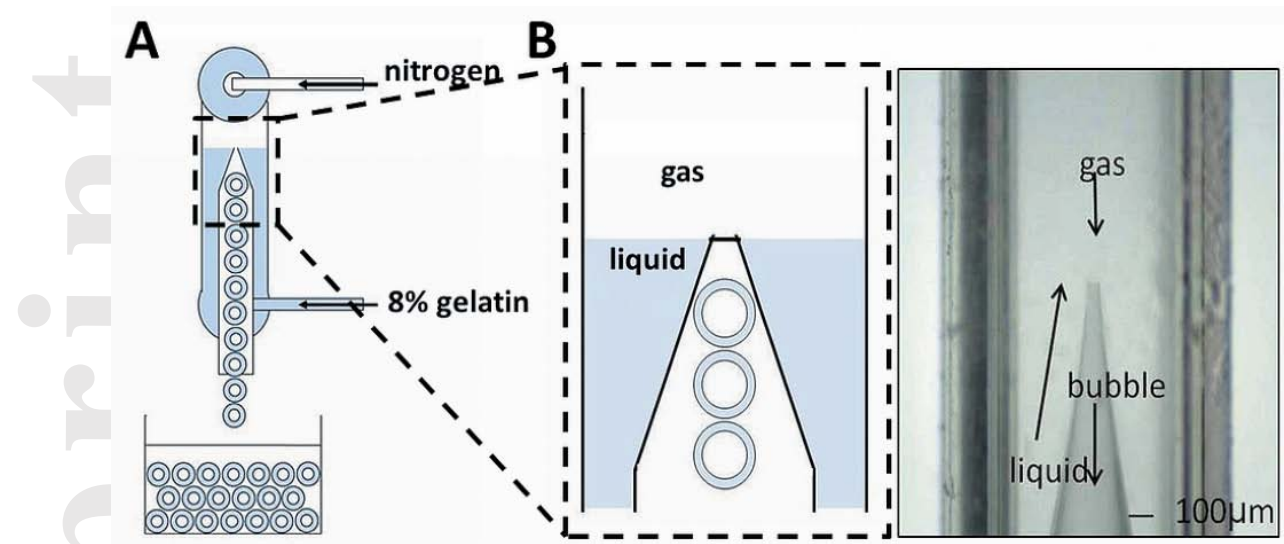


Figure 1

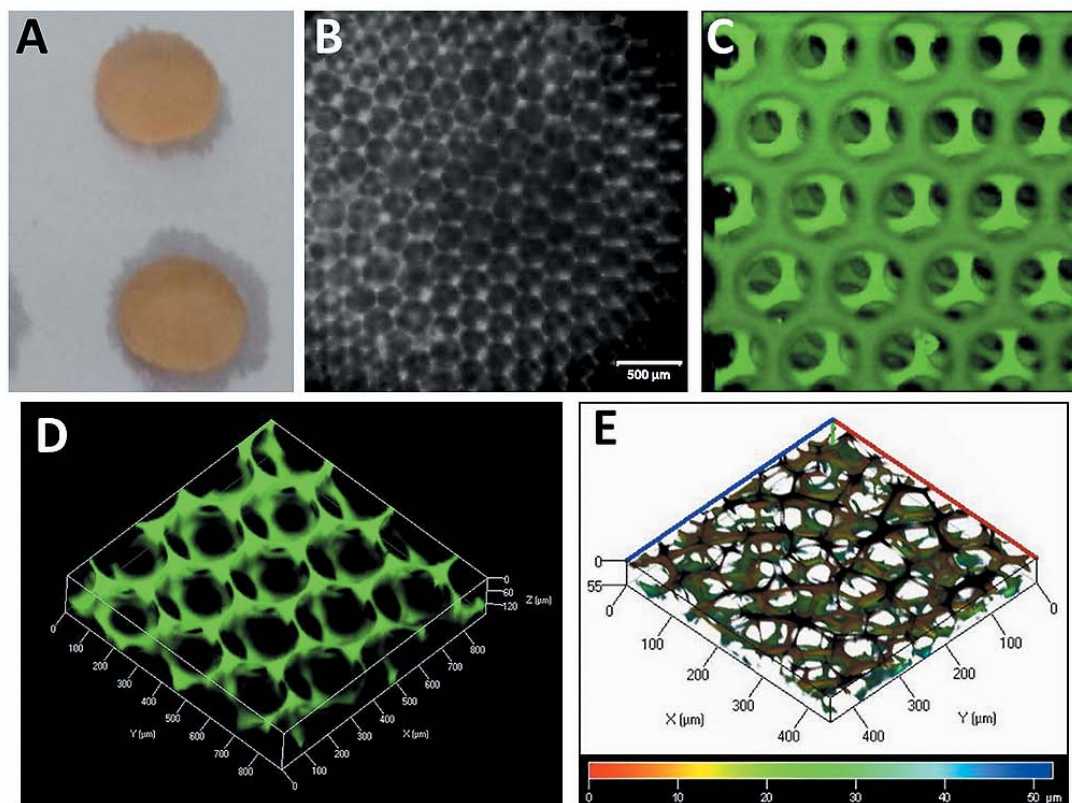


Figure 2

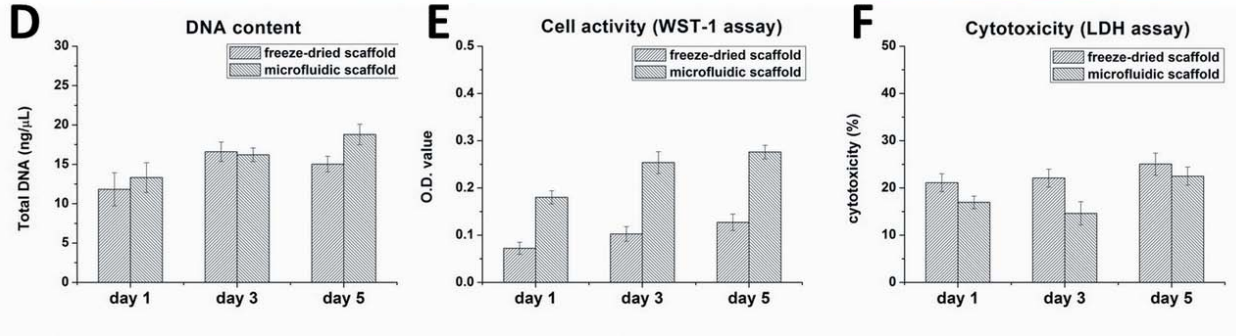
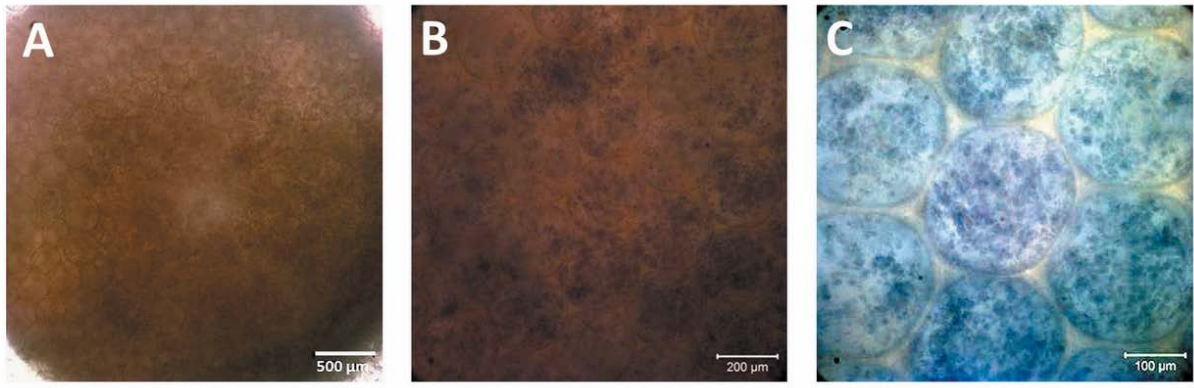


Figure 3

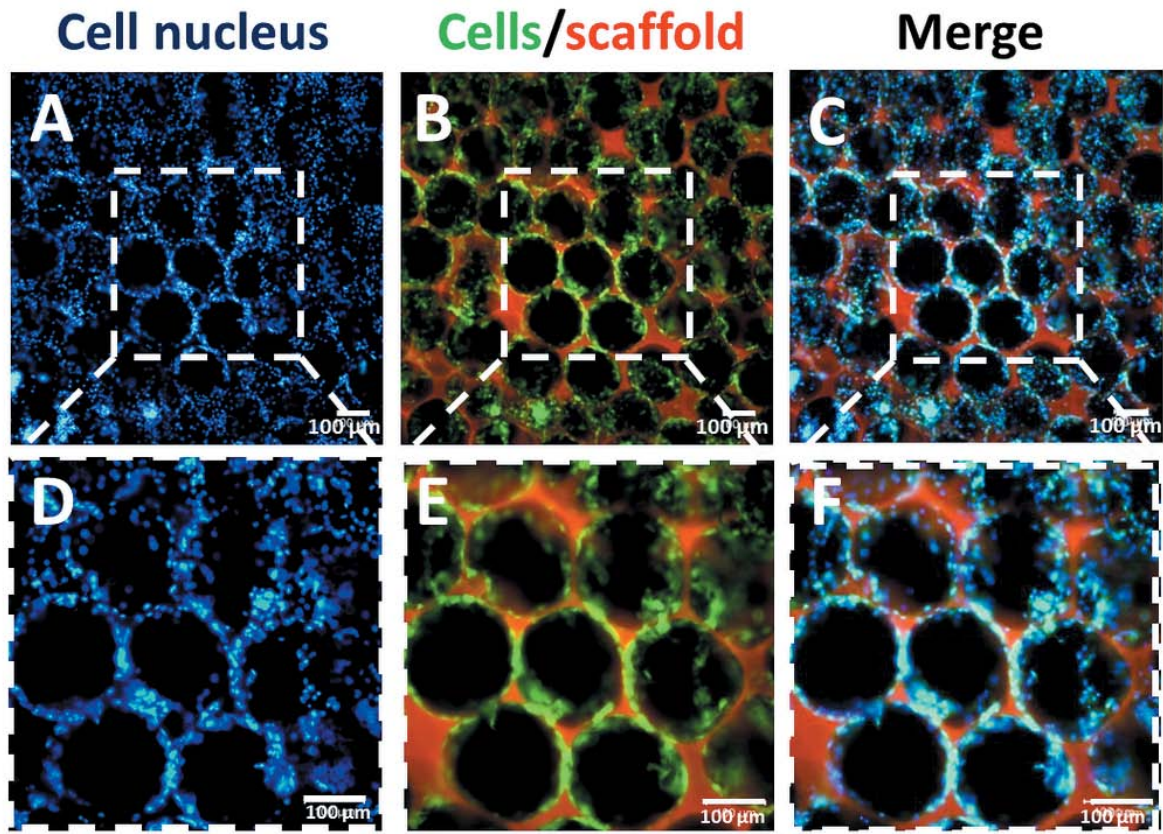


Figure 4

GAG content

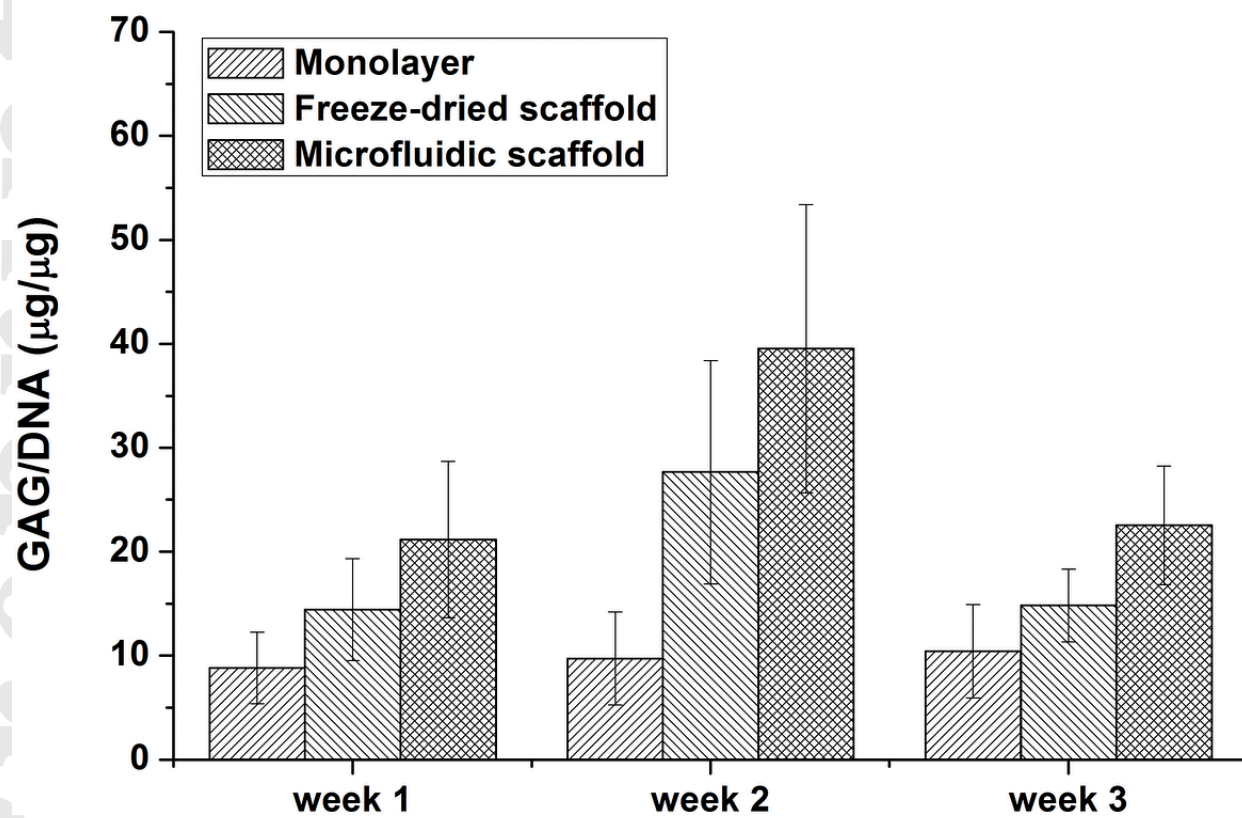


Figure 5

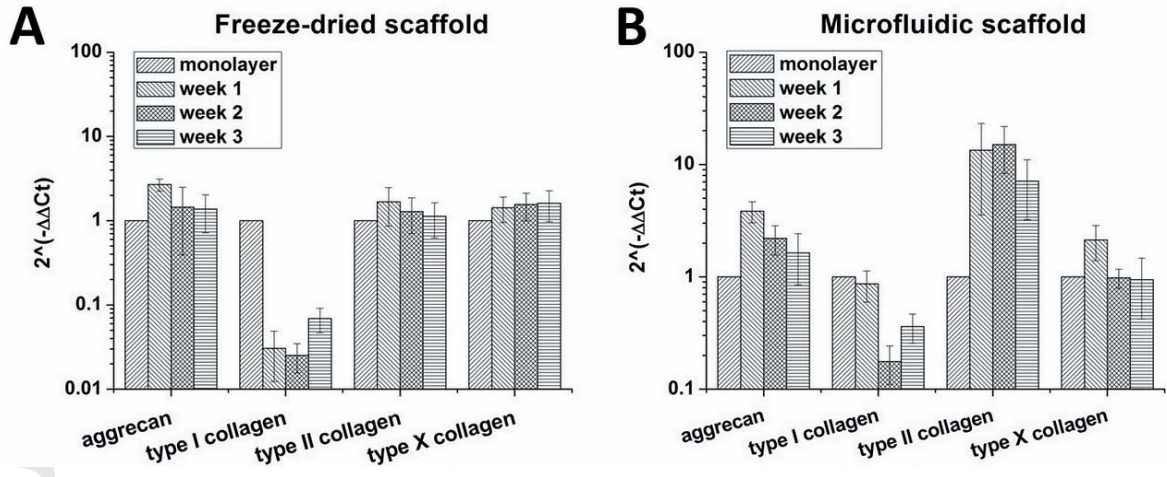


Figure 6

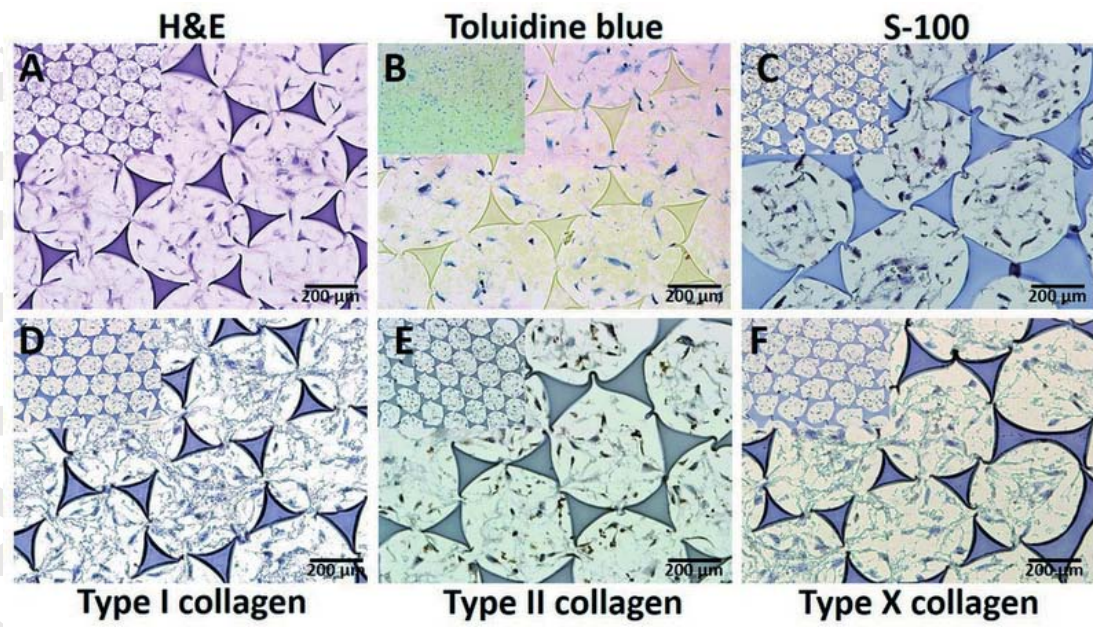


Figure 7